INTERNATIONAL JOURNAL OF ADAPTIVE CONTROL AND SIGNAL PROCESSING
Int. J. Adapt. Control Signal Process. (2012)
Published online in Wiley Online Library (wileyonlinelibrary.com). DOI: 10.1002/acs.2330

Adaptive backstepping flight control for a mini-UAV

Mihai Lungu and Romulus Lungu*,†

University of Craiova, Faculty of Electrical Engineering, 107 Decebal Blvd., Craiova, Romania

SUMMARY

The paper presents the design of a mini-unmanned aerial vehicle (UAV) attitude controller using the backstepping method. Starting from the nonlinear dynamic equations of the mini-UAV, by using the backstepping method, the authors of this paper obtained the expressions of the elevator, rudder, and aileron deflections, which stabilize the UAV at each moment to the desired values of the attitude angles. The attitude controller controls the attitude angles, the angular rates, the angular accelerations, and other variables describing the UAV longitudinal and lateral motions. The designed controller has been implemented in Matlab/Simulink environment, and its effectiveness has been tested with a campaign of numerical simulations using data from the UAV flight tests. Copyright © 2012 John Wiley & Sons, Ltd.

Received 22 March 2012; Revised 11 July 2012; Accepted 26 July 2012

KEY WORDS: backstepping; UAV; control laws; attitude angles

1. INTRODUCTION

1.1. Antecedents and motivations

All over the world, unmanned aerial vehicles (UAVs) have many civil and military applications. Many scientists design UAVs that have to meet some expectations regarding their reliability, low cost, small size, and so on and so forth. In the domain of small-size UAVs, the majority of systems are still deployed as prototypes because of their lack of reliability. Their reliability may be increased by improving their modeling and their flight control systems [1, 2]. Modeling, simulation analysis, and flight testing of full-size aircrafts or large UAVs are very well presented in lots of scientific works over the past few decades; there is not too much information regarding the modeling, simulation, and analysis of small UAV systems [3].

Many research projects have been performed for an integrated framework in recent years [4–9]. The central paradigm is a model-based development environment for the UAV where different design tools and techniques can be formulated, deployed, and applied [2]. The development of UAV flight control (Figure 1 [2]) is based on different tightly-coupled processes, and the development process will severely hindered if each process is tackled as a separate problem. The flight control design involves the dynamic modeling, the control and model analysis, simulation, control design, real-time implementation, software and hardware-in-the-loop simulation, and flight testing [2].

Most UAV autopilots use classical proportional-integral-derivative (PID) controllers and ad hoc methods to tune the controller gains during the flight. This methodology is not the best one because it has high risks and because there are many limitations in the UAVs performances and robustness. To design good controllers and to improve the system reliability and robustness, simulations through flight tests have been performed. It is important to obtain an integrated framework that enables it

*Correspondence to: Romulus Lungu, University of Craiova, Faculty of Electrical Engineering, 107 Decebal Blvd., Craiova, Romania.
†E-mail: rlungu@elth.ucv.ro

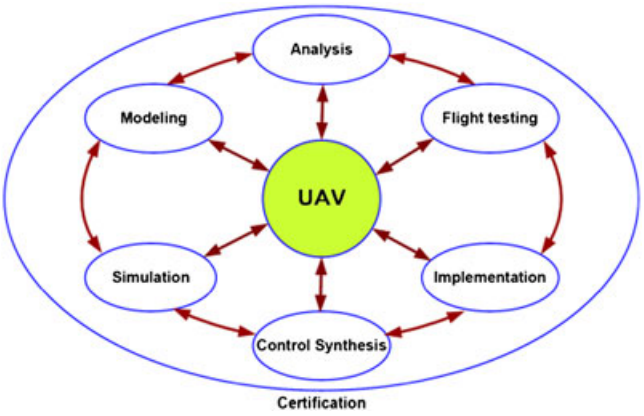

Figure 1. The integrated framework for the flight control development.

to rapidly synthesize, implement, analyze, and validate a controller configuration by using iterative development cycles [4–9].

Most of the time, the equations of the flying object motion are nonlinear. There are many techniques for the control of flying objects when their flight is described by nonlinear equations: dynamic inversion, nonlinear predictive control, or techniques that use neuronal networks [10]. By using the first method, the system nonlinearities are canceled, and a closed loop linear system is obtained. The disadvantage of this method is that we have to be completely aware of all the nonlinearities and their derivatives. This is a serious problem because the aerodynamic forces and moments, which describe the system, cannot be modeled at a high precision degree [2]. An alternative to the dynamic inversion is the backstepping method; it is a simpler method, and its most important advantage is that the nonlinearities need not to be canceled in the control law.

Feedback linearization, in its various forms, is perhaps the most commonly employed nonlinear control method; the controllers based on feedback linearization combine the aircraft's angular rates (p, q, r), the aerodynamic angles (α, β), or the Euler angles (φ, θ, ψ) as the command variables [11]. The time-scale separation means the separation of the plant dynamics into slow states and fast states, with the fast states used as virtual control for the slow ones [12]. To use the feedback linearization, all parametric plant uncertainties must appear in the same equation of the state-space representation as the control [13, 14]; this is another disadvantage of the feedback linearization method. That is why a nonlinear control method that offers relief from these issues must be used; this is the backstepping method. Backstepping makes use of a recursive procedure that breaks down the control problem for the full system into a sequence of designs for lower order systems [11, 14, 15]. The traditional backstepping method can be applied only to plants with unmatched nonlinearities, whereas the adaptive backstepping method deals with unmatched parametric uncertainties. The advantages of the backstepping method are as follows: (i) backstepping relaxes time-scale separation requirements by including transients in the virtual controls explicitly in the control formulation [2] and (ii) the designer may use Lyapunov functions as the design progresses, and he may discriminate between which nonlinearities cancel and which plant dynamics to exploit [15]. In contrast, the feedback linearization method cancels all plant nonlinearities indiscriminately. Studies of application of the backstepping method in aviation can be found in [16, 17].

An early work in the domain of the backstepping method is given by Krstic *et al.* [13]. Polycarpou obtained an extension of the adaptive backstepping by using neural networks [18, 19]; Lee and Tomizuka designed a similar method by means of fuzzy logic [20], whereas Sharma and Calise extended the study of adaptive backstepping to use a class of nonlinear-in-the-parameters neural network [21, 22].

The control of UAVs is studied, using the backstepping method, in many research papers. For example, Azinheira and Moutinho present in their paper [23] a backstepping-based controller with input saturations, applicable for the hover flight of an UAV. To cope with limitations due to reduced

DOI: 10.1002/acs

actuation, saturations are introduced in the control design, and the stability of the modified control solution is verified. Hemanshu *et al*. obtained a novel backstepping-based velocity control method for unmanned helicopters; his approach has enabled the inclusion of flapping dynamics [24]. Jung and Tsiotras consider in their work [25] the problem of path following control for a small fixed wing UAV. They use the backstepping method to derive the roll angle command by taking into account the approximate closed-loop roll dynamics. Paw used the backstepping method to the stabilization and control of a mini-UAV [11], but the used UAV has only two command surfaces (only two channels). The UAV presented in this paper has three command surfaces, and this makes the control design more difficult.

1.2. Main contribution

In this paper, the attitude controller is projected for a mini-UAV commercial off-the-shelf radio-controlled plane *Ultra Stick 25E* [2]. The UAV (Figure 2 [2]) has been made by a research group of scientists from the University of Minnesota in November 2009. The UAV has a conventional horizontal and vertical tail and three control surfaces: elevator, rudder, and ailerons. All these control surfaces are actuated by *Hitec* servos. The engine of the UAV is 600 watts *E-Flite* electric out runner motor driving an *APC* 12×6 propeller [2]. The UAV is instrumented with a suite of avionics for the flight control development research and testing. The Inertia measurement unit/Global Positioning System (IMU/GPS) sensor provides angular rates, linear accelerations, magnetic fields, airspeed, barometric altitude, GPS positions, and velocities measurement data [2, 26, 27].

The UAV dynamics, presented in this paper, was borrowed from Paw's work [2]. In [2], the stabilization of the UAV is made by a controller that has been designed by using the H_∞ technique and the μ synthesis technique. In our paper, the design of the controller is achieved by using the backstepping method. So, the main contribution of this paper is the design of the controller for the stabilization and control of the mini-UAV. There are many research papers where an adaptive backstepping controller for UAVs is designed, but there is very little research in the domain of mini-UAV controller design; our work focuses precisely on this issue. The expressions of the elevator, rudder, and aileron deflections, which stabilize the UAV at each moment to the desired values of the attitude angles, are obtained; also, the stability of the controller is demonstrated, for each of the three channels (pitch angle channel, roll angle channel, and yaw angle channel) by using six Lyapunov functions. Our work also includes an analysis of how the design constants' choice influences the stability and the performances of the system.

The paper is organized as follows: the dynamic model of the mini-UAV (six freedom degrees) is given in Section 2; the backstepping controller for the pitch angle stabilization is designed in Section 3, whereas the backstepping controller for the stabilization of the roll and yaw angles is designed in Section 4. In Section 5, the designed controller is implemented in Matlab/Simulink environment, and its effectiveness is tested with a campaign of numerical simulations using data from the UAV flight tests; the influence of the design constants on the system stability and performances is also analyzed. Finally, some conclusions are shared in Section 6.

Figure 2. The mini-UAV (Ultra Stick 25E RC plane).

DOI: 10.1002/acs

2. DYNAMIC EQUATIONS OF THE MINI-UAV

The dynamics of the mini-UAV is described by six freedom degrees [28]. The equations describing the forces (Figure 3 [2]) with respect to frame $Oxyz$ (Ox, the longitudinal axis of the UAV; Oy, the lateral axis, oriented to the right plane; Oz, the axis perpendicular on the (Oxy) plane and downward oriented) are [2] as follows:

$$\begin{aligned}\dot{u} &= rv - qw + \frac{p_d S}{m} C_X - g\sin\theta + \frac{T}{m},\\ \dot{v} &= pw - ru + \frac{p_d S}{m} C_Y - g\cos\theta\sin\varphi,\\ \dot{w} &= qu - pv + \frac{p_d S}{m} C_Z - g\cos\theta\cos\varphi,\end{aligned} \tag{1}$$

where u, v, and w are the velocity projections along the UAV frame axes; p, q, and r are the projections of the UAV angular rate $\vec{\omega}$ along UAV frame axes; $p_d = \rho V^2/2$ the UAV dynamic pressure $\left(V = \sqrt{u^2+v^2+w^2}\right)$; T is the UAV thrust force; φ, θ, and ψ are the attitude angles (roll, pitch, and yaw); S is the wing area; $\vec{g}$ is the gravitational acceleration; m is the UAV mass; and C_X, C_Y, and C_Z are the dimensionless coefficients of the aerodynamic forces $\vec{X}$, $\vec{Y}$, and $\vec{Z}$. The expressions of the aerodynamic coefficients C_X, C_Y, and C_Z are [2]

$$C_X = C_L\sin\alpha - C_D\cos\alpha,\ C_Y = C_{Y_\beta}\beta + C_{Y_{\delta_r}}\delta_r + \frac{b}{2V}\left(C_{Y_p}p + C_{Y_r}r\right),\ C_Z = -C_D\sin\alpha - C_L\cos\alpha, \tag{2}$$

where α and β are the attack angle and the sideslip angle, respectively, δ_r is the rudder deflection, b the wing span, and C_L and C_D the lift and the drag coefficients, respectively; they have the following forms [29]:

$$C_L = C_{L_0} + C_{L_\alpha}\alpha + C_{L_{\delta_e}}\delta_e + \frac{\bar{c}}{2V}\left(C_{L_{\dot{\alpha}}}\dot{\alpha} + C_{L_q}q\right),\ C_D = C_{D_0} + C_{D_{\delta_e}}\delta_e + C_{D_{\delta_r}}\delta_r + \frac{C_L - C_{L_{\min}}}{\pi\cdot e\cdot AR}; \tag{3}$$

δ_e is the elevator deflection and $\bar{c}$ is the aerodynamic mean chord.

The equations describing the projections of the moments along the $Oxyz$ frame axes are [11] as follows:

$$\begin{aligned}\dot{p} - \frac{I_{xz}}{I_x}\dot{r} &= \frac{p_d S b}{I_x} C_l - \frac{I_z - I_y}{I_x} qr + \frac{I_{xz}}{I_x} pq,\\ \dot{q} &= \frac{p_d S \bar{c}}{I_y} C_m - \frac{I_x - I_z}{I_y} pr - \frac{I_{xz}}{I_y}\left(p^2 - r^2\right) + \frac{I_e}{I_y}\Omega_e r,\\ \dot{r} - \frac{I_{xz}}{I_z}\dot{p} &= \frac{p_d S b}{I_z} C_n - \frac{I_y - I_x}{I_z} pq - \frac{I_{xz}}{I_z} qr - \frac{I_e}{I_z}\Omega_e q,\end{aligned} \tag{4}$$

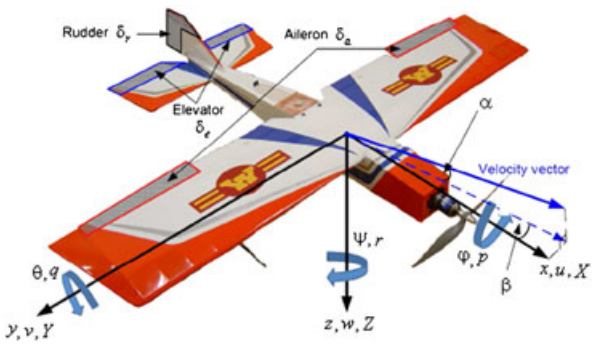

Figure 3. Forces and moments in aircraft body axis.

DOI: 10.1002/acs

with I_x, I_y, and I_z as the axial inertia moments, I_{xz} the planar inertia moment, I_e the inertia moment of the propeller, Ω_e the propeller angular rate, C_l, C_m, and C_n the aerodynamic coefficients with the expressions [2]:

$$\begin{aligned} C_l &= C_{l_\beta}\beta + C_{l_{\delta_r}}\delta_r + C_{l_{\delta_a}}\delta_a + \frac{b}{2V}\left(C_{l_p}p + C_{l_r}r\right), \\ C_m &= C_{m_0} + C_{m_\alpha}\alpha + C_{m_{\delta_e}}\delta_e + \frac{\bar{c}}{2V}\left(C_{m_{\dot{\alpha}}}\dot{\alpha} + C_{m_q}q\right), \\ C_n &= C_{n_\beta}\beta + C_{n_{\delta_r}}\delta_r + C_{n_{\delta_a}}\delta_a + \frac{b}{2V}\left(C_{n_p}p + C_{n_r}r\right). \end{aligned} \tag{5}$$

The aerodynamic coefficients have been obtained, by the research team from Minnesota, from wind tunnel tests [30], numerical computational methods [31] or flight tests for identification of the parameters [2]. To obtain these coefficients, first of all, the research team has approximated the values of the coefficients by using simulator parameters and some initial values of the coefficients from relevant work [32]. After that, the values of the coefficients have been refined using parameter identification flight tests [2]. Equation (4) is equivalent with

$$\dot{p} = \frac{I_z}{I_xI_z - I_{xz}^2}\left(C_1I_x + C_3I_{xz}\right), \dot{q} = C_2, \dot{r} = \frac{I_x}{I_xI_z - I_{xz}^2}\left(C_1I_{xz} + C_3I_z\right), \tag{6}$$

where

$$\begin{aligned} C_1 &= \frac{p_dSb}{I_x}C_l - \frac{I_z - I_y}{I_x}qr + \frac{I_{xz}}{I_x}pq, \\ C_2 &= \frac{p_dS\bar{c}}{I_y}C_m - \frac{I_x - I_z}{I_y}pr - \frac{I_{xz}}{I_y}\left(p^2 - r^2\right) + \frac{I_e}{I_y}\Omega_e r, \\ C_3 &= \frac{p_dSb}{I_z}C_n - \frac{I_y - I_x}{I_z}pq - \frac{I_{xz}}{I_z}qr - \frac{I_e}{I_z}\Omega_e q. \end{aligned} \tag{7}$$

The cinematic equations of the UAV rotations are [2]

$$\dot{\varphi} = p + \tan\theta\cdot(q\sin\varphi + r\cos\varphi), \dot{\theta} = q\cos\varphi - r\sin\varphi, \dot{\psi} = \frac{p\sin\varphi + r\cos\varphi}{\cos\theta}, \tag{8}$$

$$\theta = \gamma + \alpha\cos\varphi + \beta\sin\varphi. \tag{9}$$

In (9), γ is the slope of the flight trajectory.

3. DESIGN OF THE BACKSTEPPING CONTROLLER FOR THE PITCH ANGLE STABILIZATION

3.1. Brief presentation of the backstepping method

The main issue related to the success of autonomous UAV operations is the autopilot system for mini-UAV control, guidance, and navigation tasks. If we do not have the mathematical model of the flying object, the design of the attitude controller is difficult to be performed because the designers have to perform manual tuning of the controller gains during the flight tests with no model available. This is limited to a classical single-input, single-output controller design method, but it may also be a dangerous and time-consuming process. Some designers prefer the classical controllers because of their simplicity (the controllers are designed by successive closure of feedback loops from inner angular rate feedback loops to outer tracking loops). The design process may be difficult when more loops are added, and it requires a significant amount of time for tests and for the error tuning process; this does not guarantee the obtaining of a controller with the desired performance [2].

The backstepping method is an appreciatively new control method; it is based on the Lyapunov theory, and it offers multiple possibilities for the use of nonlinearities with respect to the dynamic inversion technique. Thus, some nonlinearities may be maintained whereas others, which are not

DOI: 10.1002/acs

necessary, are to be canceled [33]; the control law is simpler. The backstepping method is used to make the state vector, which characterizes a system, to track its desired value. The method uses fictive controls that, step by step, stabilize some variables to the values of previous fictive controls. To use the backstepping method, the differential equations describing the system must have a certain structure and, in this case, we will restrict to the strict feedback structure which is illustrated by a third-order differential equation [11]:

$$\dot{x}_1 = f_1(x_1, x_2)\ ,\ \dot{x}_2 = f_2(x_1, x_2, x_3)\ ,\ \dot{x}_3 = f_3(x_1, x_2, x_3, u)\ , \tag{10}$$

where f_1, f_2, and f_3 are nonlinear functions. In the system (10), the state x_2 is used as a virtual control to control the state x_1 to zero in the case when the dynamics of x_3 is not known. To control x_2, the state x_3 is used as a virtual control, and after that, the system input signal u is used to control the state x_3. In this case, we are having the control in a cascaded form in which a higher state is used as a virtual control of the lower state [11]. In the stability analysis, for each virtual control, a Lyapunov function is used; the design of controllers for the pitch, roll, and yaw angles can be represented by the states x_1, x_2, and x_3. The system input signal u consists of the deflections of elevator, ailerons, and rudder; the pitch, roll, and yaw angles are to be controlled by means of the angular rates, whereas the angular rates are to be controlled by means of the control input.

Let us consider a system with the general form [34]:

$$\begin{cases} \dot{x} = f_0(x) + g_0(x) \cdot z_1, \\ \dot{z}_1 = f_1(x, z_1) + g_1(x, z_1) \cdot z_2, \\ \dot{z}_2 = f_2(x, z_1, z_2) + g_2(x, z_1, z_2) \cdot z_3, \\ \vdots \\ \dot{z}_{k-1} = f_{k-1}(x, z_1, z_2, \ldots, z_{k-1}) + g_{k-1}(x, z_1, z_2, \ldots, z_{k-1}) \cdot z_k, \\ \dot{z}_k = f_k(x, z_1, z_2, \ldots, z_k) + g_k(x, z_1, z_2, \ldots, z_k) \cdot u, \end{cases} \tag{11}$$

where $x \in R^n$, $z_1, z_2, \ldots, z_k$ are scalars, u the input of the system, $f_0, f_1, f_2, \ldots, f_k$ functions taking the zero value initially $\Leftrightarrow f_i(0, 0, \ldots, 0) = 0$; and $i = \overline{0,k}$, $g_1, g_2, \cdots, g_k$ the nonzero functions in the interest domain, that is, equivalent with $g_i(x, z_1, z_2, \ldots, z_k) \neq 0$, $i = \overline{0,k}$.

Let us consider that the system described by the first equation (11) is initially stabilized by the control law $u_0(x)$,where $u_0(0) = 0$. Also, we should consider a Lyapunov function $V_0(x)$ for this stable subsystem. The determination of $u_0(x)$ can be made either by choosing the Lyapunov function $V_0(x)$ and imposing $\dot{V}_0(x, z_1) < 0$ or by means of the Sontag formula [35]. After this step, a control law $u_1(x, z_1)$ is designed such that the system described by the second equation (11) is stabilized, and z_1 tracks the desired control law $u_0(x)$; this is performed by using the Lyapunov function [34]: $V_1(x, z_1) = V_0(x) + \frac{1}{2}[z_1 - u_0(x)]^2$; $u_1(x, z_1)$ is calculated such that $\dot{V}_1(x, z_1) < 0$. Similarly, another control law $u_2(x, z_1, z_2)$ is designed such that the system described by the third equation (11) is stabilized, and z_2 tracks the desired control law $u_1(x, z_1)$. The Lyapunov function is modified again $\left(V_2(x, z_1, z_2) = V_1(x, z_1) + \frac{1}{2}[z_2 - u_1(x, z_1)]^2\right)$; $u_2(x, z_1, z_2)$ is calculated such that $\dot{V}_2(x, z_1, z_2) < 0$. The iterative process continues until the determination of u. Thus [34], u stabilizes z_k to the value of the fictive control $u_{k-1}(z_k \to u_{k-1})$; the fictive control u_{k-1} stabilizes z_{k-1} to the value of the fictive control $u_{k-2}(z_{k-1} \to u_{k-2})$; ... the fictive control u_1 stabilizes z_1 to the value of the fictive control $u_0(z_1 \to u_0)$; the fictive control u_0 stabilizes $x(x \to 0)$. The resulted system has its equilibrium point into the origin (i.e., $x \to 0$, $z_1 \to 0$, $z_2 \to 0$, ..., $z_k \to 0$), and it is an asymptotic stable system [34].

3.2. Design of the controller for the pitch channel

To stabilize the UAV pitch angle, the authors of this paper choose $\bar{\theta}$, the imposed (desired) value of the pitch angle θ, and they define the error [11]:

$$e_\theta = \theta - \bar{\theta}\,. \tag{12}$$

DOI: 10.1002/acs

From the aforementioned equation, we write $\dot{e}_\theta = \dot{\theta}$, and by using (8), we obtain the following:

$$\dot{e}_\theta = q\cos\varphi - r\sin\varphi \Leftrightarrow \dot{e}_\theta = -\mu_\theta e_\theta + \left(q + \frac{\mu_\theta e_\theta - r\sin\varphi}{\cos\varphi}\right)\cos\varphi, \tag{13}$$

with μ_θ as positive constant. The only assumption of the method is $\cos\varphi \neq 0$; our aim is $e_\theta \to 0$; this happens if $\dot{e}_\theta = -\mu_\theta e_\theta$ (the proof is based on Lyapunov stability method, and it is presented next). As a result, the term $\left(q + \frac{\mu_\theta e_\theta - r\sin\varphi}{\cos\varphi}\right)$ $\cos\varphi$ must be zero no matter how big is the roll angle value; thus, one yields

$$q = \left(-\mu_\theta e_\theta + r\sin\varphi\right)/\cos\varphi\,. \tag{14}$$

By using the relationship (14), the equation of the error e_θ becomes

$$\dot{e}_\theta = -\mu_\theta e_\theta\,. \tag{15}$$

To demonstrate that the aforementioned equation corresponds to a stable system, we choose the Lyapunov function [11]:

$$V_\theta\left(e_\theta\right) = \frac{1}{2}e_\theta^2 \tag{16}$$

and by computing $\dot{V}_\theta(e_\theta)$, it follows

$$\dot{V}_\theta\left(e_\theta\right) = e_\theta\dot{e}_\theta = -\mu_\theta e_\theta^2 < 0,\ (\forall)\,\mu_\theta > 0\,. \tag{17}$$

So, the system (15) is a stable one, and it will converge to zero $e_\theta \to 0$. The second error variable is now chosen as follows:

$$e_q = q - \bar{q}\,, \tag{18}$$

where $\bar{q}$ has the form

$$\bar{q} = \left(-\mu_\theta e_\theta + r\sin\varphi\right)/\cos\varphi. \tag{19}$$

As a result, we obtain the following equation system:

$$\begin{cases} \dot{e}_\theta = -\mu_\theta e_\theta + e_q\cos\varphi\,, \\ \dot{e}_q = \dot{q} - \dot{\bar{q}}\,. \end{cases} \tag{20}$$

Substituting $\dot{q}$,with the form (4), into the second equation (20), we find

$$\dot{e}_q = \frac{p_d S\bar{c}}{I_y}C_m - \frac{I_x - I_z}{I_y}pr - \frac{I_{xz}}{I_y}\left(p^2 - r^2\right) + \frac{I_e}{I_y}\Omega_e r - \dot{\bar{q}} \tag{21}$$

or by neglecting the term $\frac{I_e}{I_y}\Omega_e r$ ($I_e << I_y$), we obtain

$$\dot{e}_q = \frac{p_d S\bar{c}}{I_y}C_m - \frac{I_x - I_z}{I_y}pr - \frac{I_{xz}}{I_y}\left(p^2 - r^2\right) - \dot{\bar{q}}\,; \tag{22}$$

taking into account the expression of C_m (5), (22) becomes

$$\dot{e}_q = \frac{p_d S\bar{c}}{I_y}\left[C_{m_0} + C_{m_\alpha}\alpha + C_{m_{\delta_e}}\delta_e + \frac{\bar{c}}{2V}\left(C_{m_{\dot{\alpha}}}\dot{\alpha} + C_{m_q}q\right)\right] - \frac{I_x - I_z}{I_y}pr - \frac{I_{xz}}{I_y}\left(p^2 - r^2\right) - \dot{\bar{q}}\,. \tag{23}$$

Because $\dot{\alpha}$ has very small values, it can be neglected; moreover, substituting the attack angle α in (23) with the expression that derives from (9)

$$\alpha = \left(\theta - \gamma - \beta\sin\varphi\right)/\cos\varphi\,; \tag{24}$$

DOI: 10.1002/acs

under the assumption $\cos\varphi \neq 0$, the equation (23) has the following form:

$$\dot{e}_q = \frac{p_d S\bar{c}}{I_y}\left[C_{m_0} + C_{m_\alpha}\frac{\theta-\gamma-\beta\sin\varphi}{\cos\varphi} + C_{m_{\delta_e}}\delta_e\right] + \frac{p_d S\bar{c}}{I_y}\frac{\bar{c}}{2V}C_{m_q}q - \frac{I_x - I_z}{I_y}pr - \frac{I_{xz}}{I_y}\left(p^2 - r^2\right) - \dot{\bar{q}}\,. \tag{25}$$

We want to stabilize the error e_q to zero as well. For this, the following Lyapunov function

$$V_q\left(e_\theta,\, e_q\right) = \frac{1}{2}e_\theta^2 + \frac{1}{2}e_q^2 \tag{26}$$

is chosen. By computing $\dot{V}_q(e_\theta,\, e_q)$, we find

$$\begin{aligned}\dot{V}_q\left(e_\theta,\, e_q\right) &= e_\theta\dot{e}_\theta + e_q\dot{e}_q = e_\theta\left(-\mu_\theta e_\theta + e_q\cos\varphi\right) + e_q\dot{e}_q = \\ &= -\mu_\theta e_\theta^2 + e_q\left(e_\theta\cos\varphi + \dot{e}_q\right) = -\mu_\theta e_\theta^2 - \mu_q e_q^2 + e_q\left(e_\theta\cos\varphi + \mu_q e_q + \dot{e}_q\right)\,,\end{aligned} \tag{27}$$

with μ_q as positive constant. The first two terms of (27) are negative, and for this reason, it is desirable that

$$e_q\left(e_\theta\cos\varphi + \mu_q e_q + \dot{e}_q\right) = 0 \tag{28}$$

or

$$\frac{p_d S\bar{c}}{I_y}\left[C_{m_0} + C_{m_\alpha}\frac{\theta-\gamma-\beta\sin\varphi}{\cos\varphi} + C_{m_{\delta_e}}\delta_e + \frac{\bar{c}}{2V}C_{m_q}q\right] + e_\theta\cos\varphi + \mu_q e_q - \frac{I_x - I_z}{I_y}pr - \frac{I_{xz}}{I_y}\left(p^2 - r^2\right) - \dot{\bar{q}} = 0\,. \tag{29}$$

The equation of the desired elevator deflection (δ_e) results

$$\delta_e = \frac{I_y}{p_d S\bar{c}C_{m_{\delta_e}}}\left(\delta_1 - \frac{p_d S\bar{c}}{I_y}\cdot\delta_2 + \delta_3\right)\,, \tag{30}$$

with

$$\begin{aligned}&\delta_1 = -e_\theta\cos\varphi - \mu_q e_q,\ \delta_2 = C_{m_0} + C_{m_\alpha}\frac{\theta-\gamma-\beta\sin\varphi}{\cos\varphi} + \frac{\bar{c}}{2V}C_{m_q}q\,,\\ &\delta_3 = \frac{I_x - I_z}{I_y}pr + \frac{I_{xz}}{I_y}\left(p^2 - r^2\right) + \dot{\bar{q}}\,.\end{aligned} \tag{31}$$

4. DESIGN OF THE BACKSTEPPING CONTROLLER FOR THE STABILIZATION OF THE ROLL AND YAW ANGLES

The procedure is similar to the one presented previously; the authors of the paper choose $\bar{\varphi}$ as the desired (imposed) value of the roll angle and defines the error [11, 36]

$$e_\varphi = \varphi - \bar{\varphi}\,. \tag{32}$$

For $\bar{\varphi}$ as constant, it follows

$$\dot{e}_\varphi = \dot{\varphi}\,. \tag{33}$$

Introducing the expression of $\dot{\varphi}$ from (8) in (33), we find

$$\begin{aligned}\dot{e}_\varphi &= -\mu_\varphi e_\varphi + \mu_\varphi e_\varphi + p + \tan\theta\cdot(q\sin\varphi + r\cos\varphi)\\ &= -\mu_\varphi e_\varphi + \lfloor p + \left(\mu_\varphi e_\varphi + q\tan\theta\cdot\sin\varphi + r\tan\theta\cdot\cos\varphi\right)\rfloor\,.\end{aligned} \tag{34}$$

DOI: 10.1002/acs

For the convergence of error e_φ to zero, (34) must have the following form:

$$\dot{e}_\varphi = -\mu_\varphi e_\varphi \,, \tag{35}$$

where μ_φ is a positive constant. As a result, we obtain

$$p + \left(\mu_\varphi e_\varphi + q \cdot \tan\theta \cdot \sin\varphi + r \cdot \tan\theta \cdot \cos\varphi\right) = 0 \tag{36}$$

or

$$p = -\mu_\varphi e_\varphi - q \cdot \tan\theta \cdot \sin\varphi - r \cdot \tan\theta \cdot \cos\varphi \,. \tag{37}$$

Indeed, for (35), by choosing the Lyapunov function [11]

$$V_\varphi\left(e_\varphi\right) = \frac{1}{2} e_\varphi^2 \,, \tag{38}$$

we find

$$\dot{V}_\varphi\left(e_\varphi\right) = e_\varphi \dot{e}_\varphi = -\mu_\varphi e_\varphi^2 < 0, \; (\forall)\, \mu_\varphi > 0 \,. \tag{39}$$

Thus, the system is a stable one and convergent to zero $\left(e_\varphi \to 0 \Leftrightarrow \varphi \to \bar{\varphi}\right)$.

The second error variable is chosen as [11]

$$e_p = p - \bar{p} \,, \tag{40}$$

where $\bar{p}$ has the form

$$\bar{p} = -\mu_\varphi e_\varphi - q \cdot \tan\theta \cdot \sin\varphi - r \cdot \tan\theta \cdot \cos\varphi \,. \tag{41}$$

Under these conditions, we obtain the following system:

$$\begin{cases} \dot{e}_\varphi = -\mu_\varphi e_\varphi + e_p \,, \\ \dot{e}_p = \dot{p} - \dot{\bar{p}} \,. \end{cases} \tag{42}$$

Replacing $\dot{p}$ with the form in (4) into the second equation (42), it follows

$$\dot{e}_p = \frac{I_{xz}}{I_x}\dot{r} + \frac{p_d S b}{I_x} C_l - \frac{I_z - I_y}{I_x} qr + \frac{I_{xz}}{I_x} pq - \dot{\bar{p}} \tag{43}$$

or taking into account the expression of C_l (5),

$$\dot{e}_p = \frac{p_d S b}{I_x}\left[C_{l_\beta}\beta + C_{l_{\delta_r}}\delta_r + C_{l_{\delta_a}}\delta_a + \frac{b}{2V}\left(C_{l_p} p + C_{l_r} r\right)\right] + \frac{I_{xz}}{I_x}\dot{r} - \frac{I_z - I_y}{I_x} qr + \frac{I_{xz}}{I_x} pq - \dot{\bar{p}} \,. \tag{44}$$

Because $\dot{r}$ has very small values, it will be neglected; thus, we write

$$\dot{e}_p = \frac{p_d S b}{I_x}\left[C_{l_\beta}\beta + C_{l_{\delta_r}}\delta_r + C_{l_{\delta_a}}\delta_a + \frac{b}{2V}\left(C_{l_p} p + C_{l_r} r\right)\right] - \frac{I_z - I_y}{I_x} qr + \frac{I_{xz}}{I_x} pq - \dot{\bar{p}} \,. \tag{45}$$

One desires $e_p \to 0$. For this, the Lyapunov function [11]

$$V_p\left(e_\varphi, e_p\right) = \frac{1}{2} e_\varphi^2 + \frac{1}{2} e_p^2 \tag{46}$$

is chosen. By calculating $\dot{V}_p\left(e_\varphi, e_p\right)$, it results

$$\dot{V}_p\left(e_\varphi, e_p\right) = e_\varphi \dot{e}_\varphi + e_p \dot{e}_p = e_\varphi\left(-\mu_\varphi e_\varphi + e_p\right) + e_p \dot{e}_p = -\mu_\varphi e_\varphi^2 - \mu_p e_p^2 + e_p\left(e_\varphi + \mu_p e_p + \dot{e}_p\right) \,, \tag{47}$$

DOI: 10.1002/acs

with μ_p as positive constant. The first two terms of (47) are negative, and because it is desirable that $\dot{V}_p\left(e_\varphi,\, e_p\right) < 0$, we choose:

$$e_p\left(e_\varphi + \mu_p e_p + \dot{e}_p\right) = 0\,. \tag{48}$$

Replacing $\dot{e}_p$, having the form (45) in (48), the relationship (48) becomes

$$\frac{p_d S b}{I_x}\left[C_{l_\beta}\beta + C_{l_{\delta_r}}\delta_r + C_{l_{\delta_a}}\delta_a + \frac{b}{2V}\left(C_{l_p}p + C_{l_r}r\right)\right] + e_\varphi + \mu_p e_p - \frac{I_z - I_y}{I_x}qr + \frac{I_{xz}}{I_x}pq - \dot{\bar{p}} = 0 \tag{49}$$

and

$$\begin{aligned} C_{l_{\delta_r}}\delta_r + C_{l_{\delta_a}}\delta_a = {} & \frac{I_x}{p_d S b}\left(-e_\varphi - \mu_p e_p + \frac{I_z - I_y}{I_x}qr - \frac{I_{xz}}{I_x}pq + \dot{\bar{p}}\right) \\ & - \left[C_{l_\beta}\beta + \frac{b}{2V}\left(C_{l_p}p + C_{l_r}r\right)\right]. \end{aligned} \tag{50}$$

For the yaw angle stabilization, the calculus methodology is the same as previously. We choose the error variables

$$e_\psi = \psi - \bar{\psi}\,,\; e_r = r - \bar{r}\,, \tag{51}$$

where $\bar{\psi}$ is the imposed (desired) value of the yaw angle ψ, whereas $\bar{r}$ has the form

$$\bar{r} = -\mu_\psi \frac{\cos\theta}{\cos\varphi}e_\psi - \frac{\sin\varphi}{\cos\varphi}q\,. \tag{52}$$

The Lyapunov functions, which have been used, are the following ones:

$$V_\psi\left(e_\psi\right) = \frac{1}{2}e_\psi^2\,,\; V_r\left(e_\psi,\, e_r\right) = \frac{1}{2}e_\psi^2 + \frac{1}{2}e_r^2\,. \tag{53}$$

We obtain, like in the previous case (roll angle stabilization case)

$$\begin{aligned} C_{n_{\delta_r}}\delta_r + C_{n_{\delta_a}}\delta_a = {} & \frac{I_z}{p_d S b}\left(-e_\psi - \mu_r e_r + \frac{I_y - I_x}{I_z}pq + \frac{I_{xz}}{I_z}qr + \dot{\bar{r}}\right) \\ & - \left[C_{n_\beta}\beta + \frac{b}{2V}\left(C_{n_p}p + C_{n_r}r\right)\right]. \end{aligned} \tag{54}$$

The determination of rudder and ailerons deflections $(\delta_r,\, \delta_a)$ is made by solving the system formed by (50) and (54). Thus, we obtain the system:

$$\begin{cases} C_{l_{\delta_r}}\delta_r + C_{l_{\delta_a}}\delta_a = \tilde{A}_1\,, \\ C_{n_{\delta_r}}\delta_r + C_{n_{\delta_a}}\delta_a = \tilde{A}_2\,, \end{cases} \tag{55}$$

with the solution

$$\delta_r = \frac{1}{C_{l_{\delta_r}}C_{n_{\delta_a}} - C_{l_{\delta_a}}C_{n_{\delta_r}}}\left(\tilde{A}_1 C_{n_{\delta_a}} - \tilde{A}_2 C_{l_{\delta_a}}\right),\; \delta_a = \frac{1}{C_{l_{\delta_r}}C_{n_{\delta_a}} - C_{l_{\delta_a}}C_{n_{\delta_r}}}\left(-\tilde{A}_1 C_{n_{\delta_r}} + \tilde{A}_2 C_{l_{\delta_r}}\right), \tag{56}$$

where

$$\begin{aligned} \tilde{A}_1 &= \frac{I_x}{p_d S b}\left(-e_\varphi - \mu_p e_p + \frac{I_z - I_y}{I_x}qr - \frac{I_{xz}}{I_x}pq + \dot{\bar{p}}\right) - \left[C_{l_\beta}\beta + \frac{b}{2V}\left(C_{l_p}p + C_{l_r}r\right)\right], \\ \tilde{A}_2 &= \frac{I_z}{p_d S b}\left(-e_\psi - \mu_r e_r + \frac{I_y - I_x}{I_z}pq + \frac{I_{xz}}{I_z}qr + \dot{\bar{r}}\right) - \left[C_{n_\beta}\beta + \frac{b}{2V}\left(C_{n_p}p + C_{n_r}r\right)\right]. \end{aligned} \tag{57}$$

In conclusion, the authors of this paper have successfully implemented the nonlinear attitude controller on the nonlinear UAV aircraft model. The attitude controller controls the attitude angles, the angular rates, the angular accelerations, and other variables that describe the dynamics of UAV.

DOI: 10.1002/acs

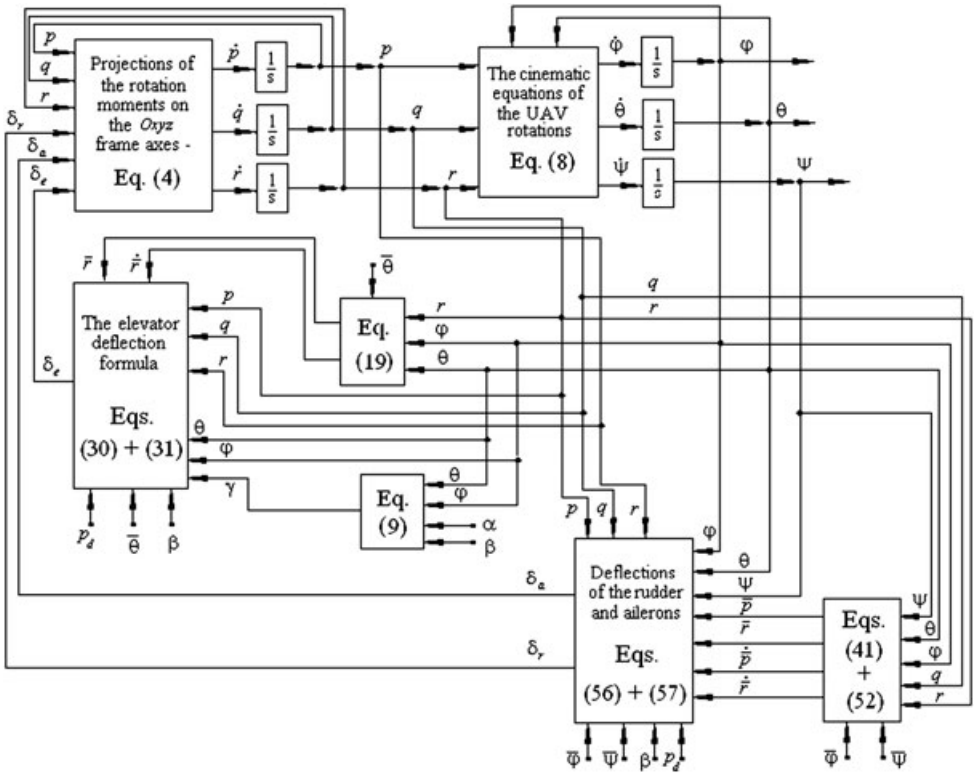

Figure 4. Structure of the attitude controller for the control of the UAV flight attitude.

The block diagram for the construction of the attitude controller (Figure 4) has been obtained by using (4), (8), (9), (19), (30), (31), (41), (52), (56), and (57).

5. SIMULATION RESULTS

In this section, we present the obtained results after performing the numeric simulations. The designed control system has been implemented in Matlab/Simulink environment, and its effectiveness has been tested with a campaign of numerical simulations. A Matlab program has been made by the authors of this paper; this program appeals complex Matlab/Simulink models for the equations presented in the previous sections. The data for simulations have been obtained from literature [2]. There are two important methods for aircraft parameter identification: identification in the time domain or in the frequency domain [2, 6, 7, 36, 37]. Here, for UAV parameter identification, the Minnesota research team used the first method because it is physically more intuitive and straightforward as the UAV dynamics is mostly represented by using time domain state-space models [2]. In Paw's work [2], the stabilization of the mini-UAV is made by using H_∞ method; this paper uses the backstepping method for the control of the UAV.

The UAV has small dimensions: the wing span is $b = 1.2$ m, the wing surface is $S = 0.32\ \mathrm{m}^2$, the mean aerodynamic chord is $\bar{c} = 0.3\ \mathrm{m}$, and its mass is $m = 1.9$ kg. We denote with H as the UAV flight altitude and with δ_T as the throttle control input; the trim conditions are very important because they are the starting values of the variables; in this simulation, the considered trim conditions are [2] as follows:

$$\begin{aligned} &u = 17\ \text{m/s}\,,\ v = 0.03\ \text{m/s},\ w = 0.37\ \text{m/s}\,,\ p = q = r = 0\ \text{deg/s}\,,\ \varphi = 0.1\ \text{deg},\ \theta = 0.25\ \text{deg},\\ &\psi = -43.6\ \text{deg}\,,\ H = 100\ \text{m},\ \Omega_e = 509\ \text{rad/s},\ V = 17\ \text{m/s},\ \alpha = 1.24\ \text{deg},\ \beta = 0.1\ \text{deg}\,,\\ &\delta_e = 9.1 \cdot 10^{-2}\ \text{rad},\ \delta_a = 1.01 \cdot 10^{-2}\ \text{rad},\ \delta_r = -6.7 \cdot 10^{-2}\ \text{rad},\ \delta_T = 42.5\%. \end{aligned} \tag{58}$$

DOI: 10.1002/acs

The aerodynamic coefficients and the inertia moments are [2] as follows:

$$\begin{aligned} &C_{m_0} = 0.135,\ C_{m_\alpha} = -1.5,\ C_{m_{\delta_e}} = -1.13,\ C_{m_{\dot{\alpha}}} = -10.4,\ C_{m_q} = -50.8\,,\\ &C_{n_\beta} = 0.0344,\ C_{n_{\delta_a}} = -0.012,\ C_{n_{\delta_r}} = -0.0345,\ C_{n_p} = -0.075,\ C_{n_r} = -0.411\,,\\ &C_{l_\beta} = -0.04,\ C_{n_{\delta_a}} = 0.0677,\ C_{n_{\delta_r}} = 0.0168,\ C_{n_p} = -0.414,\ C_{n_r} = 0.399\,,\\ &I_x = 8.94\cdot 10^{-2},\ I_y = 1.44\cdot 10^{-1},\ I_z = 1.62\cdot 10^{-1},\ I_{xz} = 1.4\cdot 10^{-2}, I_e = 1.3\cdot 10^{-4}. \end{aligned} \tag{59}$$

The imposed (desired) values of the attitude angles have been chosen as follows:

$$\bar{\varphi} = -1\,\text{deg}\,, \bar{\theta} = 3\,\text{deg}\,, \bar{\psi} = 2\,\text{deg}\,. \tag{60}$$

The Matlab/Simulink model for the attitude controller (block diagram in Figure 4) is the one in Figure 5. Time evolutions of the most important variables are presented in Figures 6–10.

In Figure 6, we present the time evolutions of the variables $\varphi(t)$, $\theta(t)$, $\psi(t)$, $p(t)$, $q(t)$, $r(t)$, $\delta_a(t)$, $\delta_e(t)$, and $\delta_r(t)$. We remark the proper function of the backstepping method because all the angles, which define the UAV attitude (the roll angle, the pitch angle, and the yaw angle), track their imposed values (60). The convergence of the attitude controllers is also confirmed by the time variations of the errors associated to the angular rates e_p, e_q, and e_r (Figure 7).

The choice of the values for the positive constants μ_φ, μ_θ ,and μ_ψ influences the responses of the system. Although the three constants are positive, the system is stable; the bigger the values of constants are, the better the system properties are (the overshoot and the transient regime period decrease). In Figures 8–10, we present the time variations of the three attitude angles for different values of the constants μ_φ, μ_θ ,and μ_ψ (values between 0.2 and 1.4). The best results are obtained

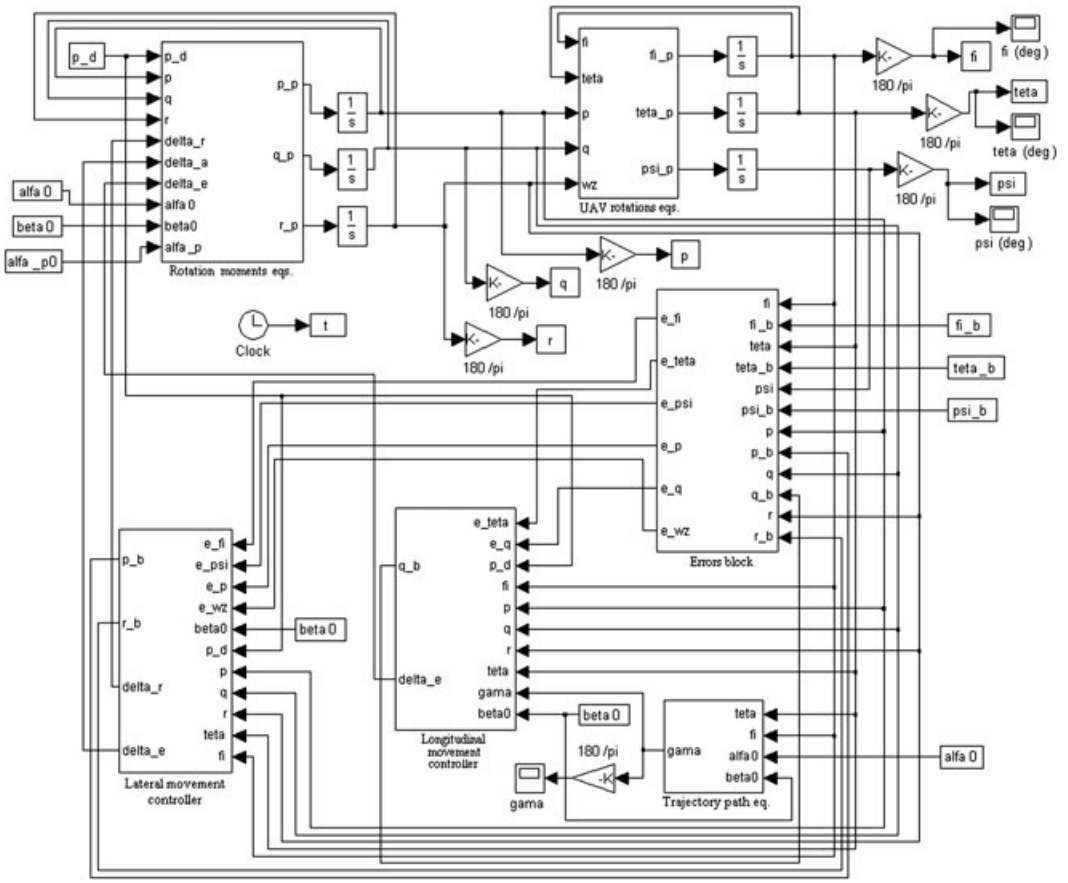

Figure 5. Matlab/Simulink model of the UAV attitude controller using the backstepping method.

DOI: 10.1002/acs

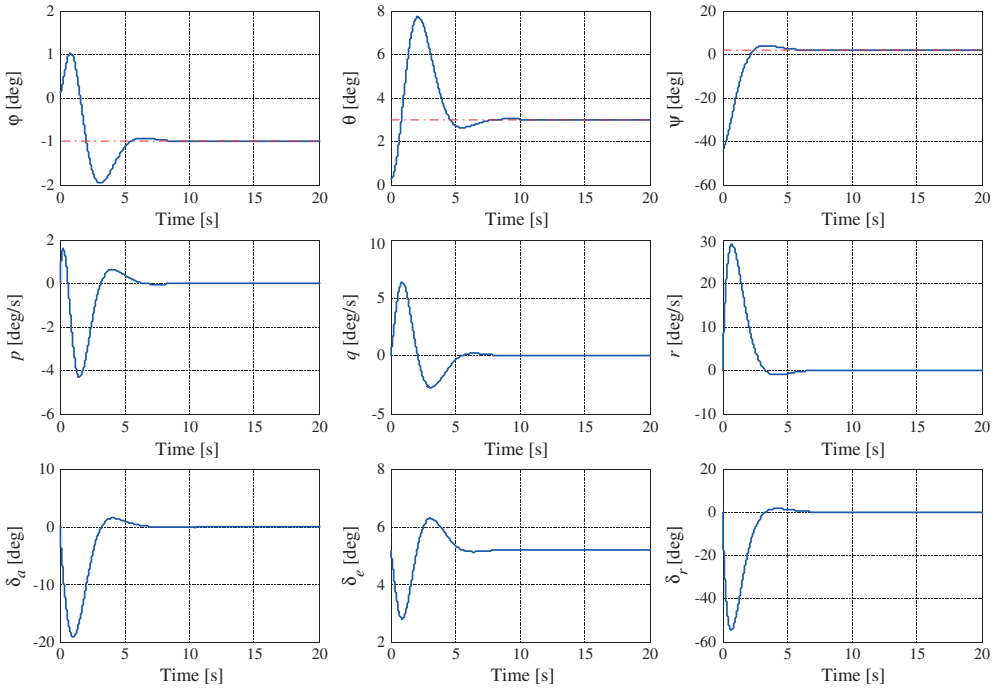

Figure 6. Time variations of the variables $\varphi(t)$, $\theta(t)$, $\psi(t)$, $p(t)$, $q(t)$, $r(t)$, $\delta_a(t)$, $\delta_e(t)$, and $\delta_r(t)$.

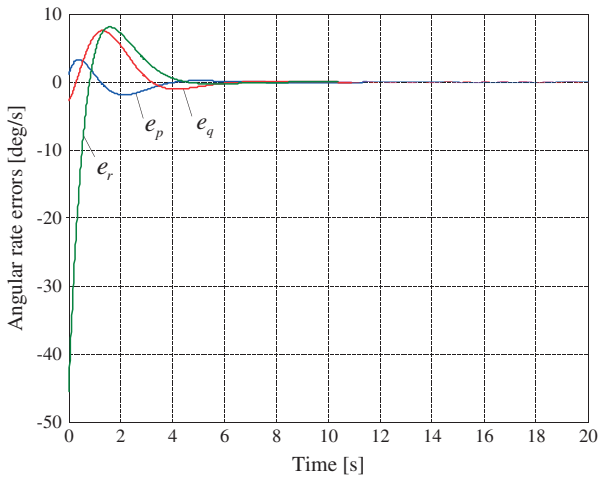

Figure 7. Time variations of the errors associated to the angular rates e_p, e_q, and e_r.

for the maximum value (in this case, 1.4). For example, if we consider the case of the roll angle stabilization, for $\mu_\varphi = 0.2$, the overshoot is -2.657 deg, whereas for $\mu_\varphi = 1.4$, it decreases to the value -1.7746 deg; that means an overshoot decrease of 33.21%. The same conclusion may be obtained regarding the transient regime period—the increase of the constant μ_φ from the value 0.2 to the value 1.4 leads to the decrease of the transient regime period from 15 to 14 s (6.67% decrease).

The obtained results are very good, and they seem to be better than the results obtained by Paw in his work [2], where the control of the same UAV was achieved by using H_∞ technique or μ synthesis technique. All these techniques provide very good results; a rigorous comparison, between these control methods for the same UAV, from the results point of view, cannot be made because we do not know if a tuning process was taken into account in Paw's work; on the other hand, the performances of our controllers (especially the transient regime and the overshoot) can be improved

DOI: 10.1002/acs

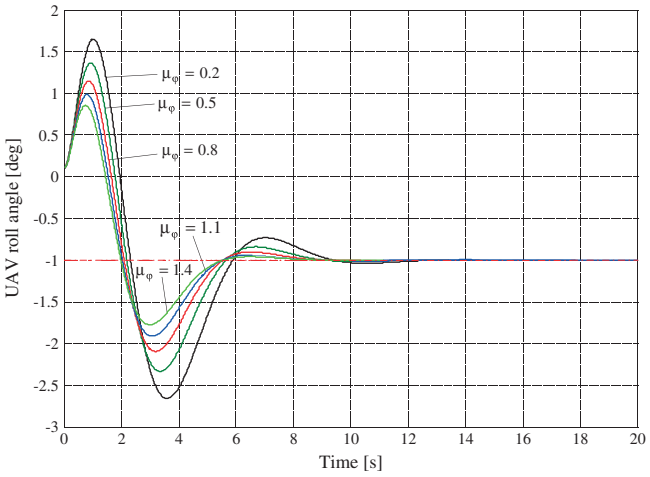

Figure 8. Time variation of the UAV roll angle for different values of μ_{φ} between 0.2 and 1.4.

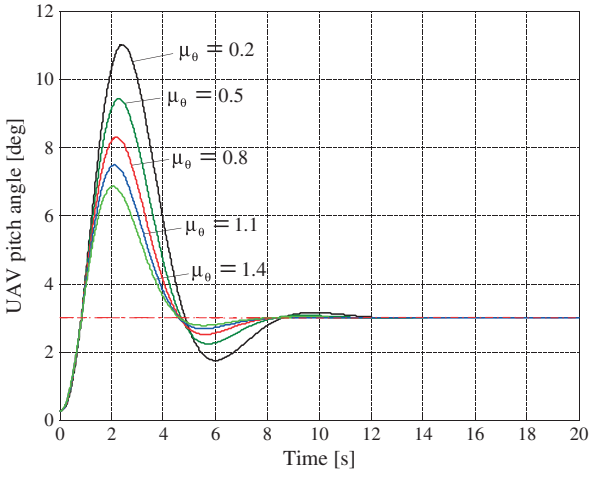

Figure 9. Time variation of the UAV pitch angle for different values of μ_{θ} between 0.2 and 1.4.

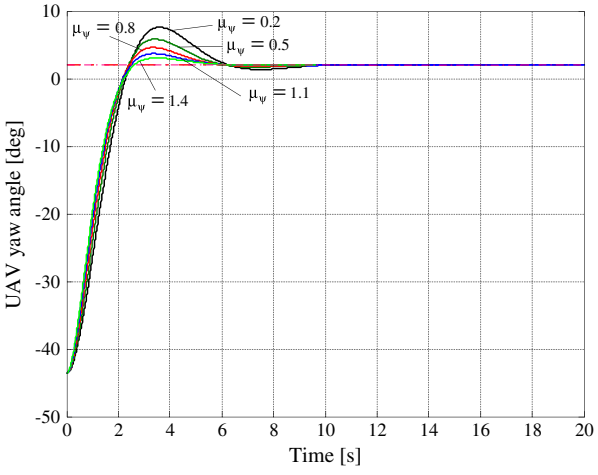

Figure 10. Time variation of the UAV yaw angle for different values of μ_{ψ} between 0.2 and 1.4.

DOI: 10.1002/acs

by increasing the values of the positive constants μ_φ, μ_θ ,and μ_ψ . However, we may conclude regarding the convergence of our backstepping controllers and regarding the obtained good results.

In [11], Paw designs a PID controller for a mini-UAV with only two command surfaces. He also designs an adaptive backstepping controller for the same mini-UAV and compares the results. The superiority of the adaptive backstepping controller is obvious. Our results are similar with the ones obtained by Paw in [11] for a different mini-UAV. Thus, if we make a brief comparison between the controllers obtained by using the backstepping method and the classical controllers (PID controllers), we remark that a classical controller has a very simple and clean feedback mechanism, whereas for the backstepping controller, there is an explosion of terms in the number of computation and feedbacks of the sensor data required to implement the controller. Therefore, to implement the controller on the embedded hardware flight computer, there might be difficulties in implementing the backstepping controller if there is limited computation power available on the flight computer. On the other hand, the backstepping controller design is a simple and straightforward design, and its main advantage is related to the fact that the nonlinear system (describing the dynamics of UAV) must not be linearized in a trim point.

6. CONCLUSIONS

The focus of the backstepping controller synthesis process was the choice of the error variables and of the Lyapunov functions. The deflections of the control surfaces have been obtained—equations (30), (31), (56), and (57). The obtained attitude controller may be implemented on UAVs; the technique that has been used for its design is a general one and may be used to all kind of flying objects, offering very good operation and characteristics of the output signals.

The backstepping technique has directly used the UAV nonlinear equations and the Lyapunov analysis. The method has an important advantage with respect to the classical techniques (for example, the design of PID controllers): the nonlinear system must not be linearized in a trim point. This linearization must be performed if we want to design PID controllers. The linearization of the UAV dynamics limits the applicability of PID controllers.

Using the backstepping method, the authors obtained the expressions of the elevator, rudder, and aileron deflections, which control the UAV at every moment and stabilize it to the desired values of the attitude angles and angular rates; viability of the approach is validated by means of complex simulations in Matlab/Simulink with data from the UAV flight tests. The obtained results are very good—the UAV attitude angles and the UAV angular rates tend to their imposed values in a proper transient regime without big overshoots. Also, the choice of the values for the positive constants μ_φ, μ_θ, and μ_ψ influences the responses of the system; the bigger values of constants are, the better the system properties are (the overshoot and the transient regime period decrease when the positive values of constants are increased).

ACKNOWLEDGEMENTS

This work was supported by the strategic grant POSDRU/89/1.5/S/61968 (2009), co-financed by the European Social Fund within the Sectorial Operational Program Human Resources Development 2007-2013.

REFERENCES

1. Chao H, Cao Y, Chen Y. Autopilots for small fixed-wing unmanned air vehicle: A survey. *IEEE International Conference on Mechatronics and Automation* 2007:3144–3149.
2. Paw YC. *Synthesis and Validation of Flight Control for UAV.* University of Minnesota, Ph.D. Dissertation, December 2009.
3. Jodeh NM, Blue PA, Waldron AA. Development of small unmanned aerial vehicle research platform: Modeling and simulating with flight test validation. *AIAA Modeling and Simulation Technologies Conference and Exhibit,* no. 2006–6261, Keystone, Colorado, 2006.
4. Jung D, Tsiotras P. Modeling and hardware-in-the-loop simulation for a small unmanned aerial vehicle. *AIAA Guidance, Navigation and Control Conference and Exhibit,* no. 2007–2768, Hilton Head, South Carolina, August 2007.
5. Kaminer O, Yakimenko V, Jones K. Rapid flight test prototyping system and the fleet of UAVs and MAVs at the naval postgraduate school. *Proceedings of the 3rd AIAA Unmanned Unlimited Technical Conference*, Chicago, Illinois, September 20–23, 2004.

DOI: 10.1002/acs

6. Corcau J, Dinca L. Comparative analysis of classical and fuzzy PI algorithms for the three-phase synchronous generator. *Proceedings of the 3rd IEEE International Symposium on Logistics and Industrial Informatics*, Budapest, 2011; 133–137.
7. Stoica AM. An H-infinity filtering problem for systems with state-dependent noise. *Control Engineering and Applied Informatics* 2009; **11**(2):35–42.
8. La Civita, Papageorgiou M, Messner G, Kanade T. Design and flight testing of a high-bandwidth H1 loop shaping controller for a robotics helicopter. *AIAA Guidance, Navigation and Control Conference and Exhibit,* no. 2002–4836, Minneapolis, United States, 13–16 August 2002.
9. Hallberg E, Komlosy J, Rivers T, Watson M, Meeks D, Lentz IK, Yakimenko O. Development and application of a rapid flight test prototyping system for unmanned air vehicle. *International Congress on Instrumentation in Aerospace Simulation Facilities*, Toulouse, France, 1999; 26.1–26.10.
10. Peyada NK, Ghosh AK. Aircraft parameter estimation using a new filtering technique based upon a neural network and Gauss-Newton method. *Aeronautical Journal* 2009; **113**:243–252.
11. Paw YC. *Attitude Control of Mini-UAV using Backstepping Control*, Nonlinear Systems Project, ME8282, October, 2007.
12. Brinker JS, Wise KA. Stability and flying qualities robustness of a dynamic inversion aircraft control law. *AIAA Journal of Guidance, Control, and Dynamics* 1996; **19**(6):1270–1277.
13. Krstic M, Kanellakopoulos I, Kokotovic P. *Nonlinear and Adaptive Control Design*. JohnWiley & Sons, Inc.: New York, 1995.
14. Khalil HK. *Nonlinear Systems*, (2nd ed.). Prentice-Hall, Inc.: New Jersey, 1996.
15. Kokotovic PV. The joy of feedback: nonlinear and adaptive. *IEEE Control Systems* 1992; **12**(3):7–17.
16. Härkegård O. Flight control design using backstepping. *Thesis No. 875*, Linköping University, 2001.
17. Härkegård O. Backstepping and control allocation with applications to flight control. *Dissertation No. 820*, Linköping University, 2003.
18. Polycarpou M. Stable adaptive neural control scheme for nonlinear systems. *IEEE Transactions on Automatic Control* 1996; **41**(3):447–451.
19. Polycarpou M, Mears MJ. Stable adaptive tracking of uncertain systems using nonlinearly parameterized on-line approximators. *International Journal of Control* 1998; **70**(3):363–384.
20. Lee H, Tomizuka M. Robust adaptive control using a universal approximator for SISO nonlinear systems. *IEEE Transactions on Fuzzy Systems* 2000; **8**(1):95–106.
21. Sharma M, Calise AJ. Adaptive backstepping control for a class of nonlinear systems via multilayered neural networks. *Proceedings of the American Control Conference*, Vol. 4, Barron Associates Inc., Charlottesville, USA, 2002; 2683–2688.
22. Sharma M. A neuro-adaptive autopilot design for guided munitions. *Ph.D. Thesis*, Georgia Institute of Technology, Atlanta, 2001.
23. Azinheira JR, Moutinho A. Hover control of an UAV with backstepping design including input saturations. *IEEE Transactions on Control Systems Technology* 2008; **16**(3):517–526.
24. Hemanshu R, Bilal A, Garratt M. Velocity control of a UAV using backstepping control. *Proceedings of the 45th IEEE Conference on Decision & Control Manchester Grand Hyatt Hotel San Diego*, CA, USA, 2006; 5894–5899.
25. Jung D, Tsiotras P. Bank-to-turn control for a small UAV using backstepping and parameter adaptation. *17th IFAC World Congress*, Seoul, South Korea, July 6–11, 2008; 4406–4411.
26. Grigorie TL. *Strap-Down Inertial Naviation Systems. Optimization Studies*. Sitech Publisher: Craiova, Romania, 2007.
27. Lungu R, Grigorie TL. *Accelerometric and Gyro Transducers*. Sitech Publisher: Craiova, Romania, 2005.
28. Nelson R. *Flight Stability and Automatic Control*. McGraw-Hill, New York City, 1997.
29. Lee YS, Vakakis AF, McFarland DM, Bergman LA. Non-linear system identification of the dynamics of aeroelastic instability suppression based on targeted energy transfers. *Aeronautical Journal* 2010; **114**(114):61–81.
30. Paw YC, Balas GJ. Uncertainty modeling, analysis and robust flight control design for a small UAV system. *AIAA Guidance, Navigation, and Control Conference*, Honolulu, HI, August 2008. AIAA-2008-7434.
31. Abdulrahim M, Lind R. Control simulation of a multi-role morphing micro air vehicle. *AIAA Guidance, Navigation and Control Conference and Exhibit*, San Francisco, CA, August 2005. AIAA-2005-6481.
32. Owens B, Cox D, Morelli E. Development of a low-cost subscale aircraft for flight research: the FASER project. *AIAA Aerodynamics Technology and Ground Testing Conference,* no. 2006–3306, San Francisco, 5–8 June 2006. 1–11.
33. Chiaramonti M, Mengali G. Control laws for a formation of autonomous flight vehicles. *Aeronautical Journal* 2009; **113**(1147):609–616.
34. Khalil HK. *Nonlinear Systems*. Prentice Hall Publisher: Upper Saddle River, NJ, USA, 2002.
35. Halgergard O. Flight control design using backstepping. *Linkoping Studies in Science and Technology Thesis No. 875*, Reglerteknik Automatic Control, Linkoping, 2001.
36. Klein V, Morelli EA. *Aircraft System Identification: Theory and Practice*. American Institute of Aeronautics & Astronautics: California, United States, 2006.
37. Jategaonkar RV. *Flight Vehicle System Identification: A Time Domain Methodology*. American Institute of Aeronautics and Astronautics: Reston, Virginia, 2006.

DOI: 10.1002/acs